

Hydrogen Energy Storage System: How does the semi-cylindrical helical coil heat exchanger affect metal hydride beds' thermal conductivity?

Puchanee Larpruenrudee^{1*}, Nick S. Bennett¹, M.J. Hossain², Robert Fitch¹, and Mohammad S. Islam¹

¹ School of Mechanical and Mechatronic Engineering, University of Technology Sydney (UTS), 15 Broadway, Ultimo, NSW-2007, Australia

² School of Electrical and Data Engineering, University of Technology Sydney (UTS), 15 Broadway, Ultimo, NSW-2007, Australia

* Email: puchanee.larpruenrudee-1@student.uts.edu.au

Abstract

Metal hydride (MH) is classified as one of the solid material storage technologies for hydrogen storage. This material has been recently used worldwide because of its ability to provide a large hydrogen storage capacity, low operating pressure and high safety. However, the disadvantage of this material is having low thermal conductivity, which leads to it having a slow hydrogen absorption time. For the absorption process, faster heat removal from the MH storage will result in faster absorption. Therefore, enhancing heat transfer performance is one of the most effective ways to improve storage performance. This paper aims to improve the heat transfer performance by employing a semi-cylindrical coil as a heat exchanger embedded inside the storage material. Air is used as the heat transfer fluid (HTF). A comparison of the hydrogen absorption duration and the bed temperature between the semi-cylindrical coil heat exchanger (SCHE) and the traditional helical coil heat exchanger (HCHE) has been made to investigate the effect of heat exchanger configuration designs. These two configurations are designed based on the constant volume of the heat exchanger tube and metal hydride. The numerical simulations are performed by using ANSYS Fluent 2020 R2. The results from this study indicate that the average bed temperature inside the storage by using SCHE is reduced faster than using HCHE, which leads to having a faster hydrogen absorption, approximately 59% time reduction. The key finding from this study could be an important enabler for industrial applications.

Keywords: Metal hydride, Hydrogen energy storage, Computational fluid dynamics, Heat transfer, Heat exchanger.

1. Introduction

Metal hydride (MH) is known as one of the solid material types suitable for hydrogen solid storage. For fuel cell applications, the MH has been recently used since it provides a higher hydrogen capacity, lower operating pressure, and lower cost compared to other options, especially liquid-state storage (Sakintuna *et al.* 2007). However, the main physical problem of the MH is having a low thermal conductivity (Zhao *et al.* 2020). This leads to having slow hydrogen absorption and desorption.

For the absorption process, faster heat removal from the storage will result in faster hydrogen absorption. Therefore, the improvement of heat and mass transfer performance is the key to improving hydrogen absorption. There are several factors that have been used to design and optimise the storage performance, including operating parameters, MH structure, and designing improved heat exchangers (Yehui *et al.* 2022). Employing cooling fluid throughout an internal heat exchanger configuration is one of the most effective ways that have been widely used. An internal straight tube was applied as the heat exchanger in several studies. By using this heat exchanger, the hydrogen absorption time (Raju & Kumar 2011) and desorption time (Chung & Lin 2009) could reduce compared to traditional MH storage. Then, a helical coil tube/spiral tube was developed as an internal



heat exchanger instead of a straight tube (Fernandez-Seara *et al.* 2014; Mellouli *et al.* 2007; Wang *et al.* 2012; Ardahaie *et al.* 2021). Because of the secondary circulations of a helical coil, that provide more surface area for the heat removal from the MH bed to the cooling fluid, the absorption time significantly improved (Wu *et al.* 2014). Wu *et al.* (2016) compared the performance of MH storage that was embedded with a straight tube, fins, and helical coil. They stated that using a helical coil as the heat exchanger obtained the best heat and mass transfer performance compared to another two cases. There was around 4000 s for the average reaction conversion of the MH as 0.40 when using a helical coil, while there were over 10000 s for the reaction conversion as 0.35 when using another two heat exchangers. Furthermore, using a double coiled tube provided better heat transfer performance compared to a straight tube, spiral tube, and straight tube incorporating with spiral tube (Tong *et al.* 2019). For 90% hydrogen concentration inside the storage, the hydrogen absorption time was reduced by 51% by using the spiral tube, while the absorption time was reduced by 73% by using a double coiled tube compared to the use of straight tube.

From the available literature, using a helical coil as a heat exchanger for the MH storage obtains an improvement in the heat and mass transfer performance rather than using a straight tube as a heat exchanger. Consequently, the aim of this study is to develop a helical coil to increase heat transfer performance. A novel semi-cylindrical tube has been developed from the traditional helical coil to be embedded inside the hydrogen energy storage device. The comparison between a semi-cylindrical tube and a helical coil tube is made to investigate the effect of these two configurations on the hydrogen absorption duration and MH bed temperature.

2. Methodology

2.1 System Description

Two MH storages with different heat exchanger configurations are presented in Figure 1. Figure 1a shows the MH storage with a helical coil heat exchanger (HCHE), while Figure 1b presents the MH storage with two semi-cylindrical coil heat exchangers (SCHE). The height and outer diameter of these storages are fixed as 100 mm and 156 mm, respectively. Air is used as heat transfer fluid (HTF) as it offers a low cost and less environmental impact. The HTF is injected from the bottom part into the porous MH storage through HCHE/SCHE, while hydrogen is injected from the top surface of the storage container. Both HCHE and SCHE are designed based on the constant volume of 100 cm³. The diameter and height of the coil tube for both cases are 146 mm and 90 mm, respectively. The tube diameter is fixed as 6 mm. The MH bed volume for both cases is 2000 cm³. The coil pitch length of HCHE and SCHE is 10 mm and 15 mm, respectively.

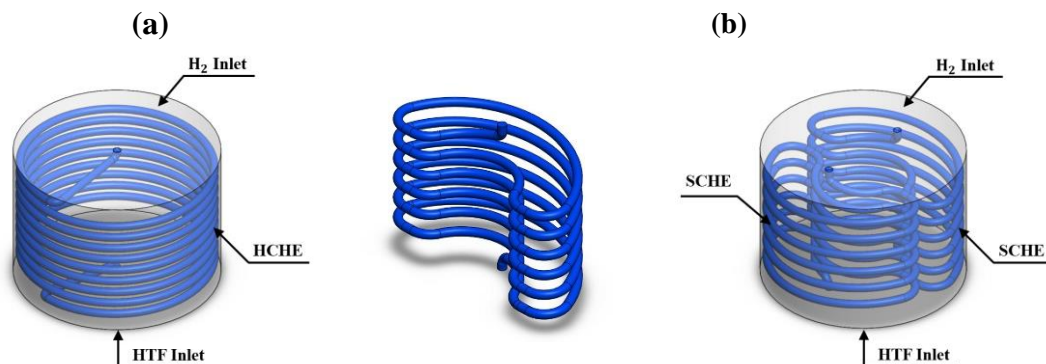


Figure 1. Geometrical characteristics of MH storage designs. (a) With HCHE, and (b) With SCHE.

2.2 Mathematical Model and Model Validation

To simplify the solution of hydrogen absorption process, the numerical simulation is performed based on some assumptions (Sekhar *et al.* 2015; Jemni *et al.* 1999; Chaise *et al.* 2010; Bao *et al.* 2013).

- Thermos-physical properties of hydrogen and MH are constant during the absorption.
- Using local thermal equilibrium conditions as the hydrogen is assumed to be an ideal gas.

- The radiative heat transfer inside the MH storage is neglected. Moreover, there is no heat transfer between the MH storage and the ambient as the storage's walls are well insulated.
- During hydrogen injection, the pressure gradient effect is negligible.

The magnesium-nickel alloy (Mg₂Ni) is selected as the metal hydride powder due to having higher hydrogen storage volume capacity and providing faster kinetics of the sorption compared to magnesium hydride and other metal hydride alloys (Rusman & Dahari 2016; Friedlmeier & Groll 1996).

ANSYS Fluent 2020 R2 was used for the numerical simulation in the present study. The source term of the energy equation was written and applied as UDFs to calculate the kinetic characteristics of the hydrogen absorption process. The energy equation for the absorption process is defined based on the thermal equilibrium between hydrogen and Mg₂Ni hydride as (Wu *et al.* 2014):

$$\frac{\partial((\rho C_p)_{e,MH} T)}{\partial t} = \nabla \cdot (\lambda_{e,MH} \nabla T) + \frac{\rho_{MH} w t (1-\varepsilon) \Delta H}{M_{H_2}} \frac{dX}{dt}, \quad (1)$$

where the effective heat capacity and conductivity are expressed as:

$$(\rho C_p)_{e,MH} = \varepsilon_{MH} \times \rho_{H_2} \times C_{p,H_2} + (1 - \varepsilon_{MH}) \times \rho_{MH} \times C_{p,MH}. \quad (2)$$

$$\lambda_{e,MH} = \varepsilon_{MH} \times \lambda_{H_2} + (1 - \varepsilon_{MH}) \times \lambda_{MH}. \quad (3)$$

where ρ_{H_2} is density of hydrogen and λ_{H_2} refers to thermal conductivity of hydrogen. C_{p,H_2} is specific heat of hydrogen and M_{H_2} is molecular weight of hydrogen. The thermo-physical properties of hydrogen can be found in Wu *et al.* (2014).

The hydrogenation reaction of the Mg₂Ni bed (ΔH) is given as:



The amount of hydrogen absorption (X) on the metal surface in wt% can be calculated from the kinetic equation in the absorption process $\left(\frac{dX}{dt}\right)$ as follows (Gambini 1994):

$$\frac{dX}{dt} = C_a \left(\frac{P_{H_2} - P_{a,eq}}{P_{a,eq}} \right) \left(\frac{x - x_f}{x_0 - x_f} \right) \exp\left(\frac{-E_a}{RT}\right), \quad (5)$$

where C_a is the reaction rate and E_a refers to the activation energy. The equilibrium pressure inside the metal hydride storage for the absorption process ($P_{a,eq}$) is determined by using the Van't Hoff equation as follows (Wu *et al.* 2014):

$$\frac{P_{a,eq}}{P_{ref}} = \exp\left(\frac{\Delta H}{RT_m} - \frac{\Delta S}{R}\right), \quad (6)$$

where P_{ref} is the reference pressure of 0.1 MPa while ΔH and ΔS are the reaction enthalpy and reaction entropy, respectively. The temperature at 573 K is selected to be the initial temperature of the MH storage as it obtains the maximum hydrogen storage capacity (3.6 wt%) of the Mg₂Ni storage (Muthukumar *et al.* 2008). Table 1 presents some major thermo-physical properties of metal hydride Mg₂Ni alloys.

Parameters	Symbols	Values
Initial temperature (K)	T_0	573
Hydrogen exerting pressure (MPa)	P_{0,H_2}	1.8
Molecular weight of MH (kg mol ⁻¹)	M_{MH}	0.1073
Hydride specific heat (J kg ⁻¹ K ⁻¹)	$C_{p,MH}$	1,414
Density of MH (kg m ⁻³)	ρ_{MH}	3,200
Density of saturated MH (kg m ⁻³)	$\rho_{SS,MH}$	3,319.32
Reaction enthalpy (J mol ⁻¹)	ΔH	-6,336
Reaction entropy (J mol ⁻¹ K ⁻¹)	ΔS	-120.84
Reaction rate constant (s ⁻¹)	C_a	175.07
Activation energy (J mol ⁻¹)	E_a	49,674
Porosity	ε	0.5
Effective thermal conductivity of MH (W m ⁻¹ K ⁻¹)	λ_{MH}	0.674

Maximum concentration of hydrogen in the MH	x_f	1.0
Initial concentration of hydrogen in the MH	x_0	0.043
Maximum mass content of hydrogen in the metal (%)	wt	3.6
Permeability (m^2)	K	1×10^{-8}

Table 1. Thermo-physical properties of hydrogen and metal hydride in model equations (Wu et al., 2014; Darzi et al., 2013).

The PRESTO scheme and PISO method are selected for the pressure-velocity coupling and pressure correction. The momentum and energy equations are solved by the second-order upwind. For the HTF, the realizable k- ϵ turbulence model is chosen with the standard wall function and other conditions, including airflow velocity as 78.75 m s^{-1} , Reynolds number as 14000, and the initial temperature as 573 K.

The grid independence has been performed to achieve reliable results based on various element sizes. The average temperature at selected locations inside the storage with HCHE becomes stable at 0.429 million elements while the average temperature of the storage with SCHE is stable at 0.431 million elements. The element sizes of 4 mm and 3 mm are used for heat exchanger tubes and MH storage, respectively. Figure 2 presents the successfully computational meshing for MH storage and two heat exchangers. The body sizing and patch conforming methods are used for mesh refinement based on the orthogonal quality metric.

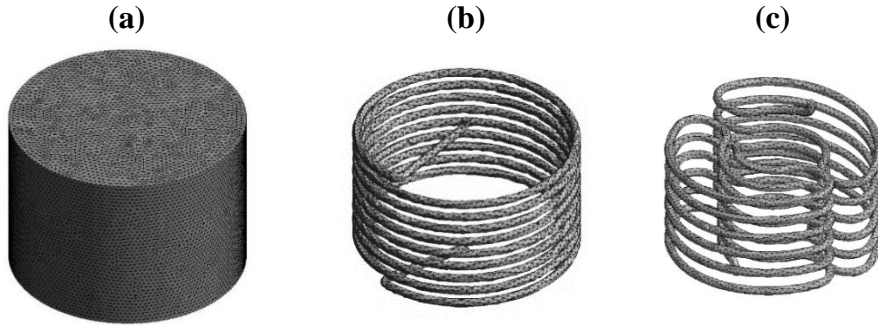


Figure 2. Computational meshing for (a) MH storage, (b) HCHE tube, and (c) SCHE tubes.

The numerical calculation of magnesium-based metal hydride storage from the present study is validated with experimental study from Muthukumar *et al.* (2008) and presented in Figure 3a. The Mg_2Ni was used as the metal hydride with a stainless-steel tube. The copper fins were employed as an internal heat exchanger. This experiment used 573 K as the initial temperature of the MH bed and 2 MPa as loading pressure. From the average bed temperature during the absorption process, it is obvious that there is a good agreement between the experimental results and numerical results.

To select an appropriate turbulence model for HTF, the results from this present study, based on various turbulence methods, are validated with the experimental results from Kumar *et al.* (2006) and presented in Figure 3b. This experimental study focused on the turbulent flow in a tube-in-tube helical heat exchanger with water as hot and cold fluids that were injected from opposite directions. The temperature of cold and hot water was 300 K and 323 K, respectively. The Dean number for the hot fluid was 550-1000, while the Dean number for the cold fluid was 3600-6000, and the Reynolds number was between 21000 to 35000. In general, the Reynolds number refers to the ratio of inertial forces to viscous forces that occur in a fluid flow. It is usually used to determine the fluid's behaviour, whether fluid flow is laminar (less than 2300) or turbulent (greater than 4000). For the Dean number, it is used to study the flow in curved pipes and channels. If the Dean number is less than 60, the flow is completely unidirectional, while if the Dean number is greater than 400, the flow is fully turbulent. From Figure 3b, it can be seen that the realizable k- ϵ turbulence model obtains more accurate results compared to other models. Thus, this model is selected for this present study.

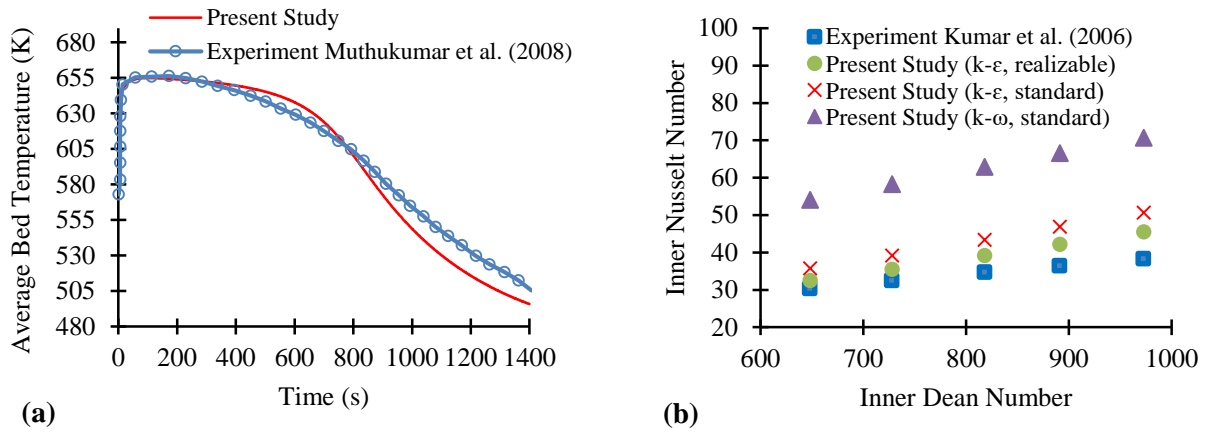


Figure 3. Model validation for (a) Code validation of the metal hydride (Mg_2Ni) storage and (b) Validation of turbulence model in helical tube.

3. Results and Discussions

The present study performs the numerical simulation of the MH storage on the hydrogen absorption process. Two SCHEs are embedded inside the MH storage to enhance the heat transfer performance. The results between the MH storage with SCHE and HCHE are then compared in terms of the average bed temperature and hydrogen concentration.

Figure 4 demonstrates the temperature at three selected points of MH storage and velocity contour for both HCHE and SCHE. These points (Figure 4a) are located at the top, middle, and bottom of the storage.

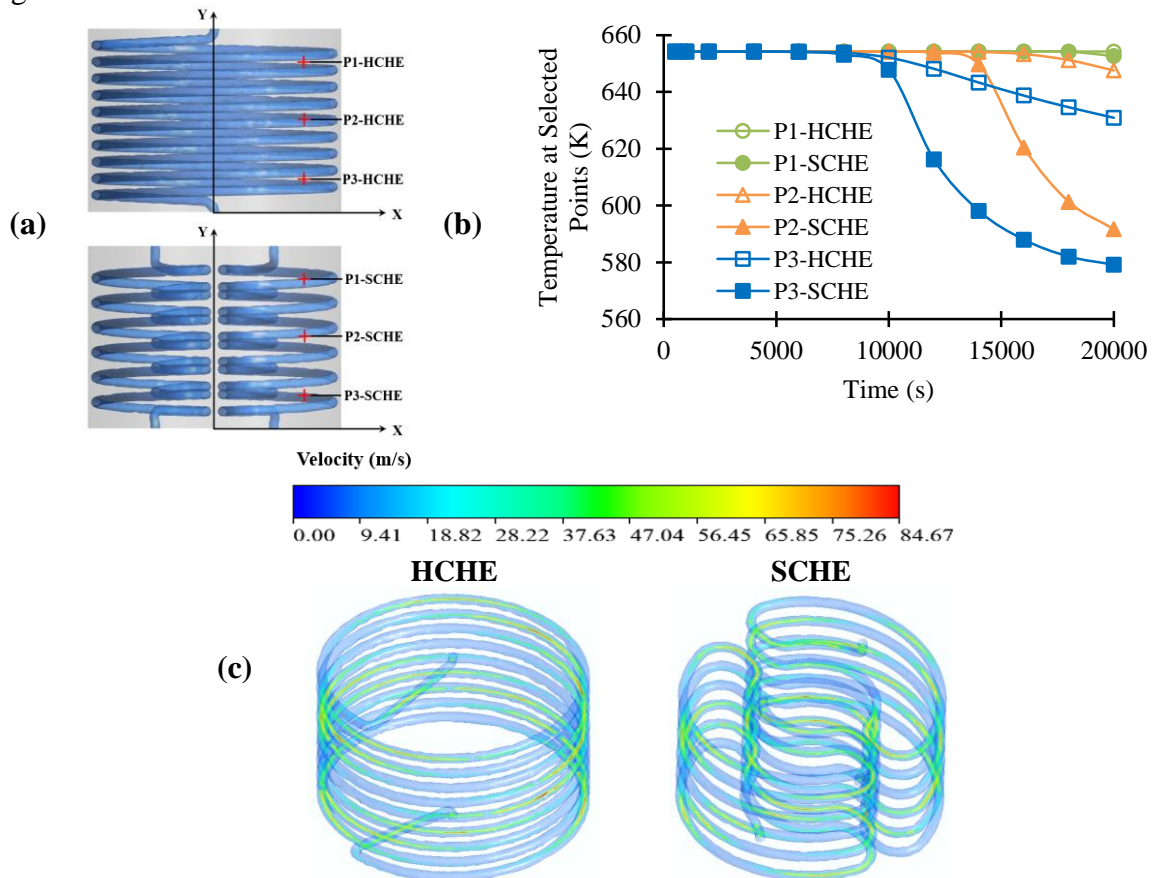


Figure 4. Temperature of MH bed at selected locations based on the incorporating with HCHE and SCHE. (a) Location of three selected points, (b) Temperature at three selected points, and (c) velocity contour for HCHE and SCHE.

From Figure 4b, it can be seen that the temperature with the case of SCHE is significantly lower than the case of HCHE, especially at P2 and P3. The temperature at the bottom part (P3) becomes lower than other parts (P1, P2), while the temperature at the top part (P1) remains stable during the whole absorption process. This is because there is a conductive heat transfer between the MH storage and HTF, which is injected from the bottom part throughout the heat exchanger tube. The temperature at P2 and P3 gradually decreases at 14000 s and 10000 s, respectively. However, this is only for the SCHE case, whereas the temperature of the HCHE case slowly decreases. At 20000 s, the temperature at P3 of the SCHE case is 579 K, while it is around 631 K at P3 of the HCHE case. The temperature at P2 from SCHE and HCHE is 592 K and 648 K, respectively. At P1, the temperature is found to be stable for the HCHE case at 654 K, while the temperature of the SCHE case is 653 K. It is clear that the temperatures at P2 and P3 are lower than 600 K for the case of SCHE, while the temperature at these points is over 630 K for the case of HCHE. The difference in temperature between these two heat exchangers is because of the well arrangement of the SCHE structure, which provides a better heat transfer surface area. The secondary circulation of the SCHE is located at the centre and nearly the wall of the storage, while the secondary circulation of the HCHE is located nearly the wall of the storage only. This leads to having a more uniform temperature distribution inside the MH storage, especially at the centre part of the SCHE case. Consequently, the temperature inside the storage from the SCHE case significantly decreases faster than in the HCHE case.

Furthermore, the velocity contour from Figure 4c also proves that the well arrangement of the SCHE structure significantly affects the turbulence level of the fluid flow. The higher velocity magnitude from the SCHE case is usually found in the curve areas, especially at the centre part of the SCHE. Therefore, a higher velocity magnitude results in a higher turbulent level in these areas, while there is no heat transfer area for the HCHE case.

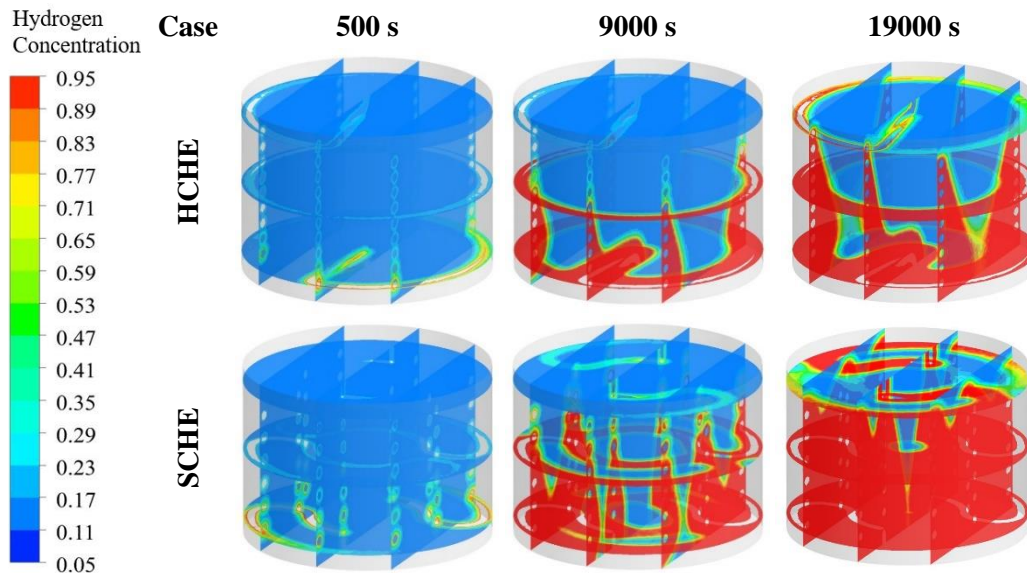


Figure 5. Hydrogen concentrations at 500 s, 9000 s, and 19000 s after starting the hydrogen absorption process for HCHE and SCHE.

Figure 5 shows the hydrogen concentrations at 500 s, 9000 s, and 19000 s after starting the absorption process. From this figure, it can be seen that the hydrogen starts to be absorbed in the bottom part of the MH storage, where it has a lower temperature (refer to P3 in Figure 4b). Nearly the entire HTF area will obtain a higher hydrogen concentration. For the case with SCHE, the hydrogen is fully absorbed in the bottom part and middle part (fully absorbed except the centre of the storage where it is far away from the HTF) of the storage. For the case of HCHE, the lower hydrogen concentration is still found at the centre of the storage and even at the bottom part of the storage. This can be explained by reasoning that using two SCHEs obtains a higher effective heat removal, which results in a lower bed temperature and faster hydrogen absorption.

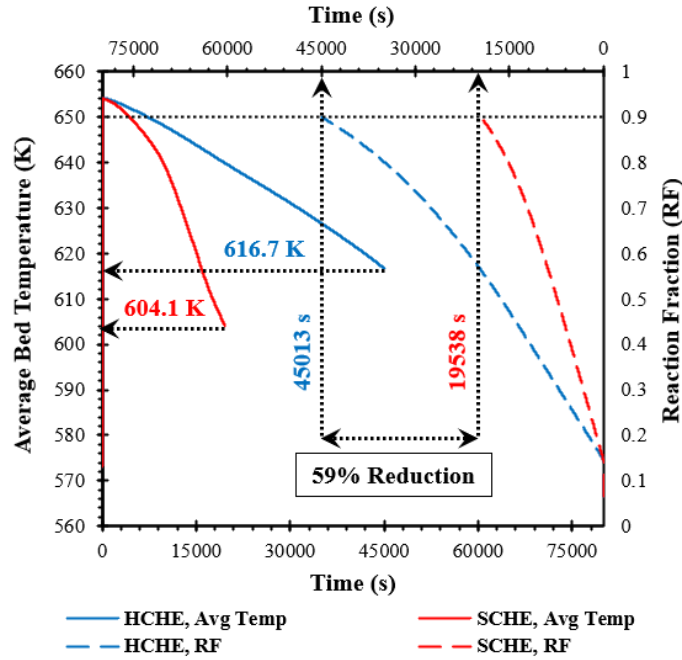


Figure 6. Reaction fraction of hydrogen coupled with average bed temperature for the MH storage with HCHE and SCHE.

Figure 6 presents the reaction fraction (RF) and average bed temperature (AVG) during the hydrogen absorption process between the case with HCHE and SCHE. Due to the exothermic behaviour of hydrogen absorption, the bed temperature rapidly increases at the beginning and continually decreases because of the conductive heat transfer between the MH bed and the HTF. For the absorption process, faster heat removal from the storage will result in faster hydrogen absorption. According to the RF, 90% RF is achieved at 19538 s when using the SCHEs, which is around 59% improvement of the hydrogen absorption duration compared to the HCHE case. This is because using the SCHEs significantly improves the heat transfer performance, resulting in better thermal conductivity inside the MH storage. The AVG using SCHE is reducing faster than using HCHE. The temperature at the final absorption by SCHE case is 604.1 K, which is lower than the HCHE case by 12.6 K.

4. Conclusions

A novel semi-cylindrical coil heat exchanger is designed and embedded inside metal hydride storage. The hydrogen absorption duration, as well as average bed temperature of the metal hydride storage, are investigated under the use of different heat exchanger configurations that have a constant volume of metal hydride bed and heat transfer fluid tube. The key findings from this present study are as follows:

- Using a semi-cylindrical coil heat exchanger increases the heat transfer area between the heat transfer fluid and metal hydride bed due to the well arrangement of the heat exchanger structure. At 90% of hydrogen absorption, the average bed temperature inside the storage with a semi-cylindrical coil heat exchanger is 12.6 K lower than the storage with a helical coil heat exchanger.
- Due to a faster temperature reduction by the use of a semi-cylindrical coil heat exchanger, the hydrogen could be absorbed faster than with the use of a traditional helical coil heat exchanger. The hydrogen absorption duration is significantly reduced by 59% by using a novel heat exchanger compared to the traditional helical coil case.
- A higher hydrogen concentration is usually found around heat transfer fluid areas as these areas have lower temperatures compared to other areas that are far away from the heat transfer fluid.

The findings from this study improve the heat transfer performance during the hydrogen absorption process of magnesium-based hydrogen energy storage incorporated with two novel semi-cylindrical coil heat exchangers. The improvement of heat transfer performance by using other heat exchanger techniques with a semi-cylindrical coil heat exchanger will be considered in the next study.

Acknowledgments

The authors acknowledge the high-performance computing facility at University of Technology Sydney (UTS).

References

- Ardahaie, S.S., Hosseini, M.J., Eisapour, M., Eisapour, A.H. & Ranjbar, A.A. 2021, A novel porous metal hydride tank for hydrogen energy storage and consumption assisted by PCM jackets and spiral tubes. *J. Clean. Prod* **311**, 127674
- Bao, Z., Yang, F., Wu, Z., Cao, X. & Zhang, Z. 2013, Simulation studies on heat and mass transfer in high-temperature magnesium hydride reactors. *Appl. Energy* **112**, 1181–1189.
- Chaise, A., Rango, P.D., Marty, P. & Fruchart, D. 2010, Experimental and numerical study of a magnesium hydride tank. *Int. J. Hydrogen Energy* **35**, 6311–6322.
- Chung, C. & Lin, C.S. 2009, Prediction of hydrogen desorption performance of Mg₂Ni hydride reactors, *Int J Hydrogen Energy* **34**, 9409–9423.
- Darzi, A.R., Farhadi, M., Sedighi, K., Aallahyari, S. & Delavar, M.A. 2013, Turbulent heat transfer of Al₂O₃water nanofluid inside helically corrugated tubes: numerical study. *Int. Commun. Heat Mass Tran* **41**, 68-75.
- Fernandez-Seara, J., Pi neuro-Pontevedra, C. & Dopazo, J.A. 2014, On the performance of a vertical helical coil heat exchanger. Numerical model and experimental validation. *Appl Therm Eng* **62**, 680-689.
- Friedlmeier, G. & Groll, M. 1996, *Proceedings International Symposium on Metal Hydrogen Systems, Switzerland, August 25–30*, 497–507.
- Gambini M. 1994, Metal hydride energy systems performance evaluation. Part A: dynamic analysis model of heat and mass transfer. *Int. J. Hydrogen Energy* **19**, 67-80.
- Jemni, A., Ben Nasrallah, S. & Lamloumi, J. 1999, Experimental and theoretical study of a metal–hydrogen reactor. *Int. J. Hydrogen Energy* **24**, 631–644.
- Kumar, V., Saini, S., Sharma, M. & Nigam, K.D.P. 2006, Pressure drop and heat transfer study in tube-in-tube helical heat exchanger. *Chem. Eng. Sci.* **61**, 4403–4416.
- Mellouli, S., Askri, F., Dhaou, H., Jemni, A. & Nasrallah, S.B. 2007, A novel design of a heat exchanger for a metal-hydrogen reactor. *Int. J. Hydrogen Energy* **32**, 3501-3507.
- Muthukumar, P., Prakash Maiya, M., Srinivasa Murthy, S., Vijay, R. & Sundaresan, R. 2008, Tests on mechanically alloyed Mg₂Ni for hydrogen storage. *J. Alloys Compd.* **452**, 456–461.
- Raju, M. & Kumar, S. 2011, System simulation modeling and heat transfer in sodium alanate based hydrogen storage systems. *Int. J. Hydrogen Energy* **36**, 1578-1591.
- Rusman, N.A.A. & Dahari, M. 2016, A review on the current progress of metal hydrides material for solid-state hydrogen storage applications. *Int. J. Hydrogen Energy* **41**, 12108–12126.
- Sakintuna, B., Lamari-Darkrim, F. & Hirscher, M. 2007, Metal hydride materials for solid hydrogen storage: a review. *Int. J. Hydrogen Energy* **32**, 1121-1140.
- Sekhar, B.S., Lototskyy, M., Kolesnikov, A., Moropeng, M.L., Tarasov, B. & Pollet, B. 2015, Performance analysis of cylindrical metal hydride beds with various heat exchange options. *Journal of Alloys and Compounds* **645**, 89–95.
- Tong, L., Xiao, J., Yang, T., B´enard, P. & Chahine, R. 2019, Complete and reduced models for metal hydride reactor with coiled-tube heat exchanger. *Int. J. Hydrogen Energy* **44**, 15907–15916.
- Wang, H., Prasad, A.K. & Advani, S.G. 2012, Hydrogen storage system based on hydride materials incorporating a helical-coil heat exchanger. *Int. J. Hydrogen Energy* **37**, 14292-14299.